Microstructure and property enhancement of silicon nitride-barium aluminum silicate composites with β-Si$_3$N$_4$ seed addition

Bo Wang · Jun Yang · Rui Guo · Jiqiang Gao · Jianfeng Yang

Abstract Si$_3$N$_4$-barium aluminum silicate (BAS) self-reinforced composites have been prepared by pressureless sintering at 1800 °C for 2 h. The β-Si$_3$N$_4$ seeds incorporated in the starting α-Si$_3$N$_4$ powders encouraged the α- to β-Si$_3$N$_4$ phase transformation, and the final bimodal microstructure with large grains, consequently, led to the improvement of the fracture toughness, from 7.74 to 8.34 MPa m$^{1/2}$. The almost-complete crystallized BAS benefited the high-temperature mechanical properties. The residual stress, crack deflection, grain bridging, and pullout were considered as the major toughening mechanisms in this composite.

Introduction

Silicon nitride ceramics are used in numerous applications because of their superior mechanical properties [1–4]. However, Si$_3$N$_4$ components have high manufacturing costs and poor reliability, which are major barriers to their extensive applications [1–4]. Generally, gas pressure sintering (GPS) or hot pressing (HP) is essential to help densification of silicon nitride ceramics and for promoting the α-Si$_3$N$_4$ to β-Si$_3$N$_4$ phase transformation, hence resulting in the formidable price of the silicon nitride

components. Pressureless sintering offers a lower fabrication cost approach, and is necessary for the wide practical application of silicon nitride materials.

Si$_3$N$_4$ is difficult to be densified without the use of sintering additives, primarily because of the highly covalent bond character. Although many oxide additives have been successfully demonstrated to produce dense Si$_3$N$_4$, the additives end up as a grain-boundary glass phase, which degrades the properties at high temperature. Therefore, a good additive system should form a liquid phase at a low liquid eutectic temperature, which subsequently is crystallized completely into a compound with a high melting point. Barium aluminum silicate (BAS) has one of the highest melting temperatures (1760 °C) among the glass-ceramic materials [5], and the monoclinic form exhibits a low thermal expansion coefficient [6]. Therefore, BAS is attracting considerable attention for the use as structural and electronic components as well as matrix for ceramic-matrix composites [6–8]. Pickup et al. [9, 10] investigated the densification behavior and mechanical characterization of BaO–Al$_2$O$_3$–SiO$_2$ system as sintering aid for silicon nitride. The resulting dense Si$_3$N$_4$ with a predominantly crystalline intergranular phase BaAl$_2$Si$_2$O$_8$ exhibited excellent high-temperature strength. In recent years, considerable attention has been devoted to BAS by ceramics because of its potential application as a matrix in ceramic-matrix composites [11–14]. Weight fractions as high as 30% were used, in contrast to the amounts of sintering additives normally added to conventional Si$_3$N$_4$ ceramics, which is usually 10–15%. We expect that these large quantities of BAS will more strongly influence the composite properties than would the sintering additives.

However, further toughness improvement is still necessary to achieve the practical use. Recent research results have shown that rod-like β-Si$_3$N$_4$ could be grown in situ

B. Wang (✉) · J. Yang · R. Guo · J. Gao · J. Yang
State Key Laboratory for Mechanical Behavior of Materials,
Xi'an Jiaotong University, Xianning West Road No. 28,
Xi'an City, Shaanxi Province 710049,
People's Republic of China
e-mail: xiaoboking@gmail.com

J. Gao
e-mail: jqgao@mail.xjtu.edu.cn

from α-Si_3N_4 in the presence of liquid BAS [12, 15–17]. Addition of β-Si_3N_4 seeds has also shown to be quite effective to improve fracture toughness because of a bridging or a crack-deflection toughening by the abnormally grown β-Si_3N_4 grains [18, 19]. This study intends to produce BAS/Si_3N_4 composites by pressureless sintering process with the addition of special β-Si_3N_4 seeds, and evaluate the role of β-Si_3N_4 seeds on the density, α- to β-Si_3N_4 phase transformation, microstructure, and mechanical properties of BAS-Si_3N_4 composites.

Experimental procedure

Preparation of BAS

$BaCO_3$ (purity >99%) was mixed with 32 wt.%SiO_2 (purity >99%) and 27.1 wt.% Al_2O_3 (purity >99%) powder by wet milling in anhydrous alcohol for 24 h in a plastic bottle. After milling, the slurry was dried, and the obtained powder mixture was sieved, and sintered at 1300 °C for 2 h to obtained BAS. The BAS powders were subsequently pulverized and screened through a 150 μm screen.

Preparation of rod-like β-Si_3N_4 seeds

α-Si_3N_4 powder (0.5 μm) and β-Si_3N_4 powder (Grade SN-P21FC, Denkikagaku, Tokyo, Japan) were used as the starting powders, Y_2O_3 (99.9% purity) and MgO (99.9% purity) were used as the sintering additives and the addition contents are 5 wt.% and 2 wt.%, respectively. The above starting powder mixture was wet milled with high-purity Si_3N_4 balls in anhydrous alcohol for 24 h in a plastic bottle. After milling, the slurry was dried, sieved, and heated in a furnace (High multi-5000, Fujidempa Co. Ltd., Osaka, Japan) at 1800 °C for 1 h under a nitrogen pressure of 0.6 MPa. The heated powder was milled and then subjected to acid rinse treatments to remove the residual glassy phase.

Sintering of BAS/Si_3N_4 composites

The starting powder mixture containing α-Si_3N_4 (0.5 μm), 30 wt.% BAS, and 5 wt.%β-Si_3N_4 seeds powders was wet milled with high-purity Si_3N_4 balls in anhydrous alcohol for 24 h in a plastic bottle. The slurry was dried in a rotary evaporator and ground with an alumina mortar and pestle followed by sieving through a 150 μm screen. The mixed powders were then uniaxially pressed to form rectangular bars measuring 30 mm · 30 mm · 5 mm. The green blocks were placed in BN-coated graphite crucibles embedded in Si_3N_4 and BAS mixed powders, and sintered in a furnace (High Multi-5000 Fijidempa Co. Ltd., Osaka, Japan) at 1800 °C for 2 h under a nitrogen pressure of 0.6 MPa.

Crystalline phases of the resultant samples were identified by XRD (D/MAX-2400X, Rigaku Co., Tokyo, Japan) analysis. The specimens were machined into test bars for flexural strength measurement. The flexure strength was measured by three-point bending method with a 20 mm span at a crosshead speed of 0.5 mm/min at room temperature. The fracture toughness was determined by single-edge-notched-beam (SENB) method at room temperature with 20 mm span at a crosshead speed of 0.05 mm/min. Each final value was averaged over six measurements. The density of specimens was determined by Archimedes method. The theoretical density of the specimens was calculated according to the rule of mixtures. The microstructure was characterized by SEM (JSM-35C, JEOL, Tokyo, Japan) and TEM (JEM-200CX), and the intergranular phases were analyzed by using the selected-area electron diffraction (SAED). The TEM specimens were prepared by cutting and grinding the sintered specimen to a plate with a thickness of 20 μm, and then dimpling and ion beam milling.

Results and discussion

Phase transformation and densification

Typical X-ray diffraction patterns for the seed-free and 5 wt.% β-Si_3N_4 seeds reinforced 30%BAS/Si_3N_4 composites are shown in Fig. 1. Primarily β-Si_3N_4 and hexacelsian $BaAl_2Si_2O_8$ phases were identified in the composite with seeds, whereas a trace of residual α-Si_3N_4 phase was detected in the composite sintered without seeds. The heterogeneous nucleation is the dominant mechanism in the α- to β-phase transformation during the liquid-phase sintering of Si_3N_4 [20–22]. The observation of an increase in β-phase content with the addition of β-Si_3N_4 seed suggested a decrease in activation energy for reprecipitation of β-phase on the seeds. Therefore, these particles were effective seeds in the sense that they acted as nuclei for α-β transformation because the transformation kinetics was faster in the seeded specimens. The crystalline BAS phase present in all cases was of the hexacelsian modification. The hexacelsian BAS underwent a destructive transformation at approximately 300 °C. However, the presence of more rode-like β-Si_3N_4 grains had a tendency to preclude the hexacelsian to orthorhombic transformation in 30%BAS/Si_3N_4 [12, 23]. The density of the samples sintered with seeds was determined as 3.15 g/cm^3, which had slightly decreased, in comparison to 3.20 g/cm^3 for the samples sintered without seeds, because of the large elongated grains in the matrix which lowers the driving force for the densification when β-seeds are available for the reprecipitation and growth of β-phase [24].
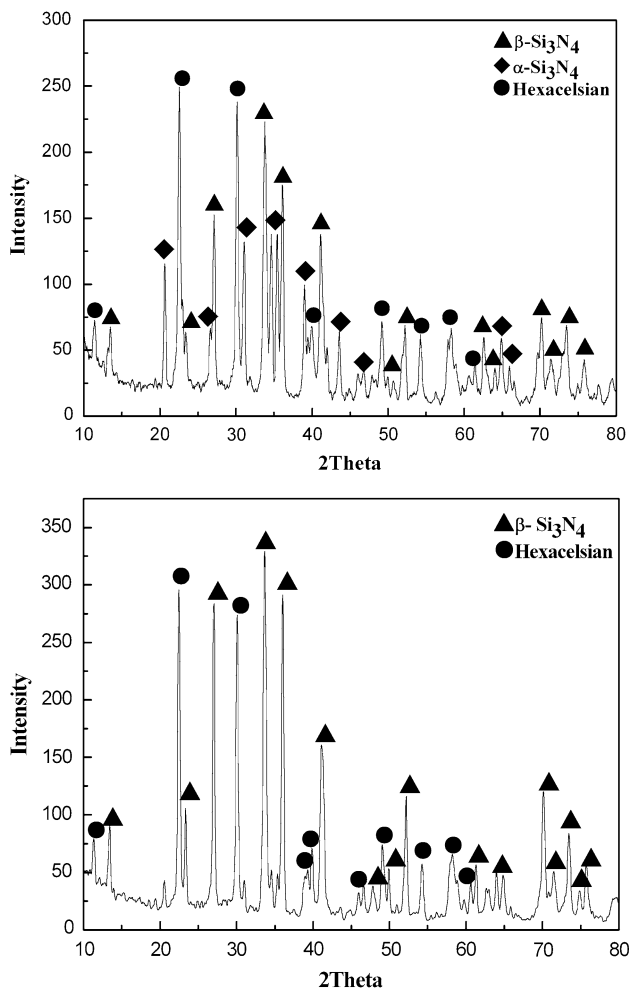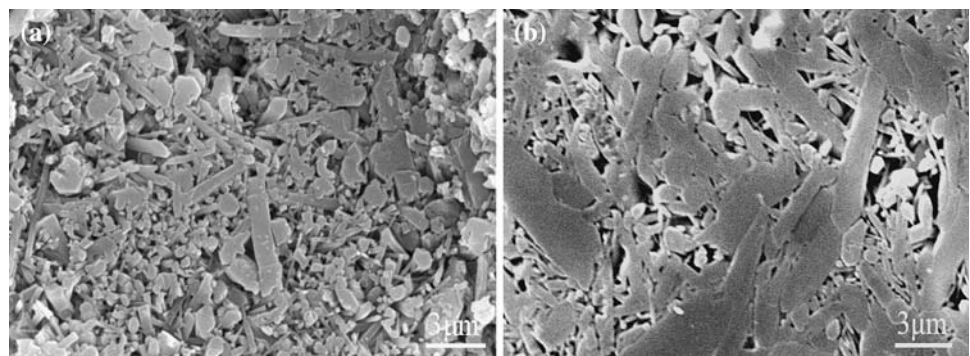
Fig. 1 XRD patterns of 30%BAS/Si$_3$N$_4$; sample was sintered at 1800 °C for 1 h. **a** seed free **b** with 5 wt.% β-Si$_3$N$_4$ seeds

Microstructural characterization

The microstructures of unseeded and seeded 30%BAS/Si$_3$N$_4$ ceramics after pressureless sintering are shown in Fig. 2. Samples were over-etched by melted NaOH to reveal the β-Si$_3$N$_4$ grains distribution. Nonseeded specimens exhibited a relatively uniform microstructure composed of randomly distributed, small, elongated grains with diameters of several tenths of a micrometer and lengths of a few micrometers, as shown in Fig. 2a. On the other hand, Seeding at 5 wt.% led to the formation of many large elongated grains (Fig. 2b). A distinct bimodal microstructure was obtained in which a small amount of reinforced Si$_3$N$_4$ grains, which have high aspect ratio embedded in smaller grains and the elongated β-Si$_3$N$_4$ grains were oriented randomly in a continuous BAS matrix. The elongated β-Si$_3$N$_4$ with abnormal grain growth had width larger than 1 μm with a high aspect ratio of >6. This bimodal microstructure exhibited high anisotropy and is expected to benefit the fracture toughness, because of the elongated β-Si$_3$N$_4$ grains which contribute to crack deflection and bridging. Such microstructural evolution of seeded specimens was reflected by the fact that small matrix grains were grown from β-Si$_3$N$_4$ particles present in the starting Si$_3$N$_4$ powder, whereas large, elongated grains developed from rod-like seed particles [25].

Typical TEM micrograph of 30%BAS/Si$_3$N$_4$ with 5 wt.% β-Si$_3$N$_4$ seeds is shown in Fig. 3a. After sintering at 1800 °C for 2 h, well-defined β-Si$_3$N$_4$ grains embedded in a completely wet crystalline matrix of barium aluminosilicate. Although similar in contrast, this phase could be distinguished from the β-Si$_3$N$_4$ phases by its wetting, non-faceted nature. This microstructures exhibited high anisotropy, where large, elongated β-Si$_3$N$_4$ grains, almost lying within the same plane, were preferentially oriented parallel to BAS, which sometimes grew in bundles [26]. In some regions, the microstructure composed randomly distributed, small, elongated grains was complex. Figure 3b shows the β-Si$_3$N$_4$ grain boundary between grain pockets. The grain boundary appeared to be straight and well defined, having a very thin film thickness. Like other silicon nitride materials [27, 28], Moire fringes were observed at some specific angles, which suggested the existence of misfit strain at the interface, as a result of the compositional difference. Using HRTEM methods, Fig. 3c shows that very thin amorphous films, typically <2 nm, were present

Fig. 2 SEM micrograph of 30%BAS/Si$_3$N$_4$ **a** seed free, **b** with 5 wt.% β-Si$_3$N$_4$ seeds; sample was sintered at 1800 °C for 2 h

Fig. 3 **a** TEM micrograph of 30%BAS/Si$_3$N$_4$ with 5 wt.% β-Si$_3$N$_4$ seeds; sample was sintered at 1800 °C for 2 h; **b** the morphology of hexagonal Si$_3$N$_4$ grains; **c** grain-boundary glassy phase; **d** a crystalline boundary phase present at a grain pocket; **e** EDS spectra of the BAS from the three grains in (**d**)
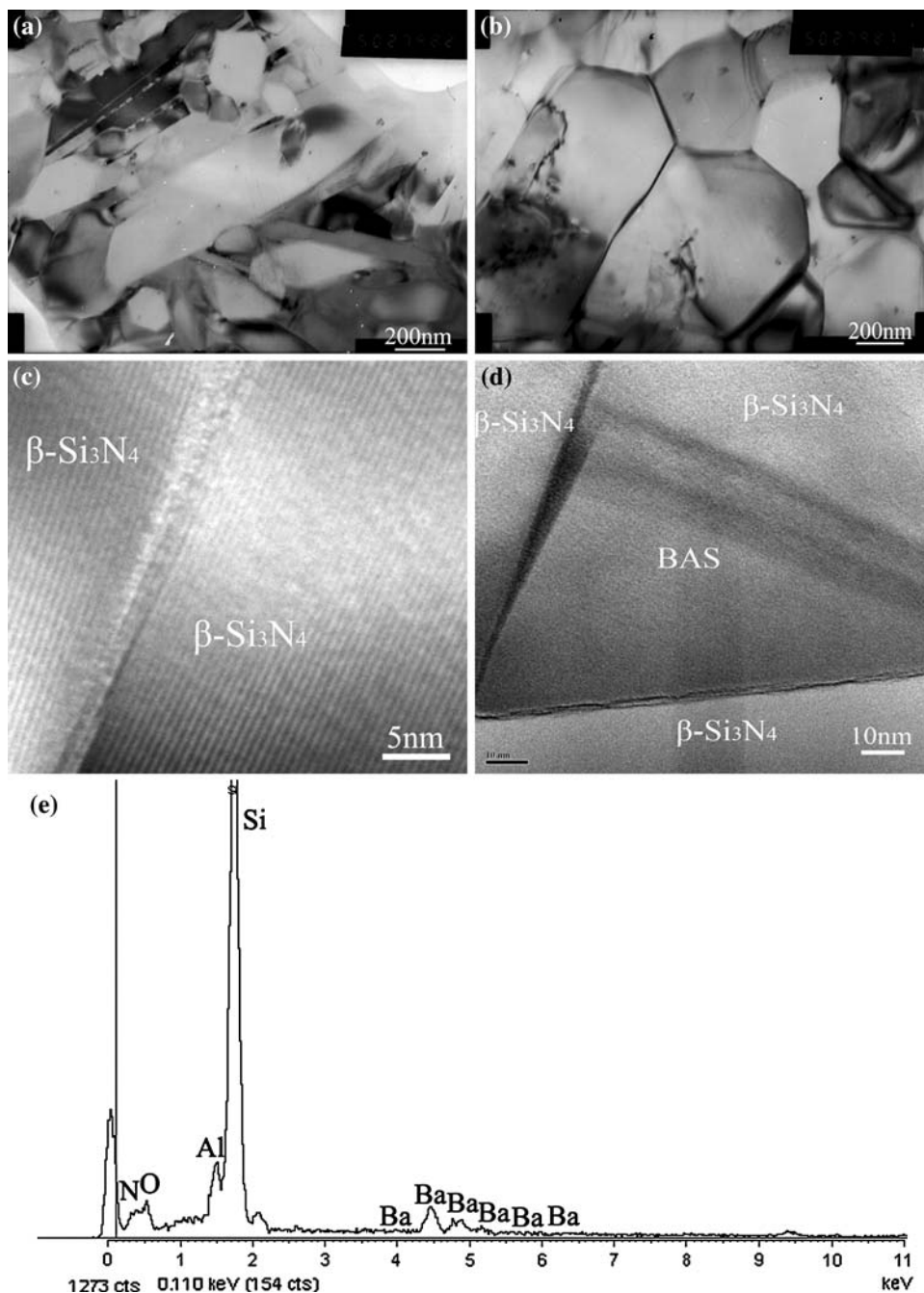
at the grain boundaries. Areas such as these were assumed to be residual from an incomplete crystallization of BAS. Within the resolution capability of HRTEM, the thickness was almost constant. Also, different sintering procedures did not seem to change the characteristics of this thin film [16]. Figure 3d shows a crystallized pocket between silicon nitride grains with the barium aluminosilicate phase in the inner part of the pocket. Microdiffraction analysis indicated this phase to be crystalline, and energy dispersive spectral (EDS) analysis from the wetting intergranular phase revealed the presence of significant barium and aluminum indicative of the expected barium aluminosilicate, as shown in Fig. 3e. The almost-complete crystallization of the BAS matrix in this composite illustrates an important advantage for its high temperature application. Heterophase grain boundaries between silicon nitride and the crystallized BAS also show amorphous grain boundary films, which often exhibit a larger thickness than the films between silicon nitride grains. In addition, a large variation of film thickness was observed.
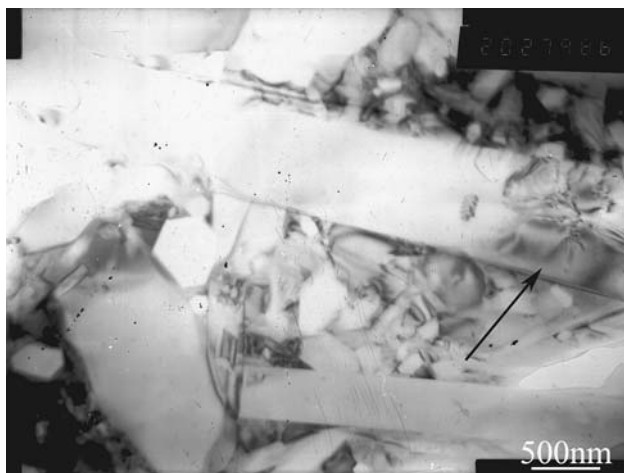
Fig. 4 TEM micrograph of abnormal elongated grains of 30%BAS/Si$_3$N$_4$ with 5 wt.% β-Si$_3$N$_4$ seeds; sample was sintered at 1800 °C for 2 h

Figure 4 is the TEM micrograph of an elongated β-Si$_3$N$_4$ grain. The complex dislocation structure and subgrain boundary was observed in the elongated Si$_3$N$_4$ grain, as indicated by the arrow. As previously reported by Lu et al. [29], the large, elongated grains possibly were formed by the coalescence of two neighboring subgrains with a very small disorientation, ≤1°. This dislocation at the junction of two subgrains was probably a result of the difference of thermal explanation coefficient between the two grains and the stacking defects at coalescence.

Mechanical properties

The mechanical properties of the investigated 30 wt.% BAS/Si$_3$N$_4$ composites are shown in Fig. 5. The average K$_{IC}$ of the 30 wt.%BAS/Si$_3$N$_4$ composites reinforced by
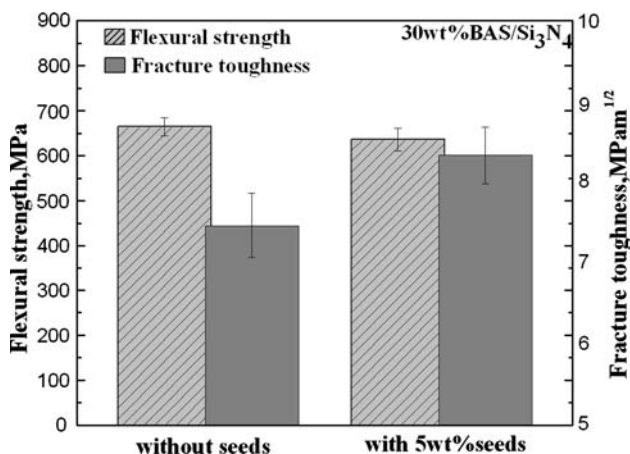
5 wt.% rod-like β-Si$_3$N$_4$ seeds increased from 7.47 to 8.34 MPa m$^{1/2}$, and the flexure strength slightly decreased from 665 to 636 MPa. Silicon nitride often suffered a very substantial loss in strength with increase in grain size, because the grain boundaries of larger grains may act as initiation sites of larger flaws. In this study, the flexural strength could be maintained at mostly the same level. This result indicated that the achievement of both high fracture toughness and high strength in this composite was made possible through encouraging bimodal microstructure with the abnormal grain growth by pressureless sintering process with the addition of special β-Si$_3$N$_4$ seeds, where the size and content of large grain were controlled within a certain range.

The high fracture toughness is undoubtedly attributed to the high concentration of large rod-like β-Si$_3$N$_4$ grains of the bimodal microstructure. On the other hand, the coefficient of thermal expansion (CTE) of hexagonal BAS (8×10^{-6} °C) significantly exceeds that of β-Si$_3$N$_4$ (3.3×10^{-6} °C) [30], so it will cause residual tensile stress at the interface and compressive stress in Si$_3$N$_4$ grain after cooling to room temperature. This thermal mismatch stress most likely contributes to the promotion of crack deflection, the formation of bridging grains, and also the enhancement of whisker pullout [31]. A model based on CTE mismatch was developed by Taya et al. [32] to explain the influence of the residual stresses on the toughness of particulate-reinforced ceramic–matrix composites, which confirmed that the residual stress is the main toughening mechanism for this glass-ceramic composite. The typical fracture surface of the composite obtained after flexural strength test is shown in Fig. 6. Grain pullout, crack bridging, and crack deflection feature, which are known toughening mechanisms for brittle materials, were exhibited.
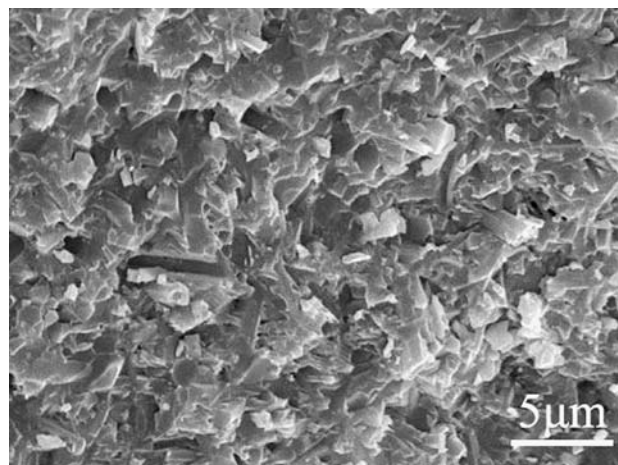

Fig. 5 Effect of the β-Si$_3$N$_4$ seeds on the mechanical properties of 30 wt.%BAS/Si$_3$N$_4$; sample was sintered at 1800 °C for 2 h

Fig. 6 Fracture surface of 30%BAS/Si$_3$N$_4$ with 5 wt.% β-Si$_3$N$_4$ seeds; sample was sintered at 1800 °C for 2 h

Conclusions

Dense 30 wt.%BAS/Si$_3$N$_4$ self-reinforced composite is synthesized by pressureless sintering. The BAS nearly completely crystallized to hexacelsian BaAl$_2$Si$_2$O$_8$ in triple-grain junctions. The grain-boundary amorphous film was observed along the entire grain boundary. The addition of β-Si$_3$N$_4$ seeds encourages the α- to β-Si$_3$N$_4$ phase transformation and determine the size of the abnormally grown grains in the final microstructure. The improvement of fracture toughness was directly related to the bimodal microstructure with large grains in the fine matrix grains, which arose from the residual stress, grain pullout, crack bridging, and crack deflection.

References

1. Riley FL (2000) J Am Ceram Soc 83:245
2. Sajglik P, Dusza J, Hoffmann MJ (1995) J Am Ceram Soc 78:2619. doi:10.1111/j.1151-2916.1995.tb08031.x
3. Liu HH, Huang JL (2001) Ceram Int 27:621. doi:10.1016/S0272-8842(01)00008-6
4. Hayashi T, Munakata H, Suzuki H, Saito H (1986) J Mater Sci 71:3501. doi:10.1007/BF02402994
5. Drummond CH, Lee WE, Bansal NP, Hyatt MJ (1989) Ceram Eng Sci Proc 10:1485. doi:10.1002/9780470310588.ch64
6. Bandyopadhyay A, Aswarth PB (1995) Mater Res 10:3143. doi:10.1557/JMR.1995.3143
7. Jang HM, Kim KS, Jung CJ (1992) J Am Ceram Soc 75:2883. doi:10.1111/j.1151-2916.1992.tb05524.x
8. Ye F, Zhou Y, Lei TC, Yang JM, Zhang LT (2001) J Mater Sci 36:237. doi:10.1023/A:1004830229429
9. Pickup H, Brook RJ (1987) Br Ceram Proc 39:69
10. Pickup H, Brook RJ (1986) In: Bunk W, Hausner H (eds) Proc 2nd Int Symp Ceramic Materials and components for Engines, p 93
11. Freitag DW (1995) Mater Sci Eng A 195:197. doi:10.1016/0921-5093(94)06519-5
12. Bandyopadhyay A, Aswath PB, Porter W, Cavin OB (1995) J Mater Res 10:1256. doi:10.1557/JMR.1995.1256
13. Bandyopadhyay A, Quander SW, Aswath PB, Freitag DW, Richardson KK, Hunn DL (1995) Scr Metall Mater 72:1417. doi:10.1016/0956-716X(95)00181-T
14. Richardson KK, Freitag DW, Hunn DL (1995) J Am Ceram Soc 72:2662. doi:10.1111/j.1151-2916.1995.tb08037.x
15. Hwang CJ, Newman RA (1996) J Mater Sci 31:150. doi:10.1007/BF00355139
16. Drummond Ch (1990) J Non-Cryst Solid 123:114
17. Fang Y, Yu F, White KW (2000) J Mater Sci 35:2695. doi:10.1023/A:1004749825368
18. Kanzaki S, Brito ME, Valecillos MC, Hirao K, Toriyama M (1997) J Eur Ceram Soc 17:1841. doi:10.1016/S0955-2219(97)00081-2
19. Hirosaki N, Akimune Y, Mitomo M (1994) J Am Ceram Soc 77:1093. doi:10.1111/j.1151-2916.1994.tb07277.x
20. Becher PF (1991) J Am Ceram Soc 74:255. doi:10.1111/j.1151-2916.1991.tb06872.x
21. Hirao K, Nagaoka T, Brito ME, Kanzaki S (1996) J Ceram Soc Jpn 104:54
22. Becher PF, Sun EY, Plucknett KP, Alexander KB, Hsueh CH, Lin HT et al (1998) J Am Ceram Soc 81:2831
23. Quander SW, Bandyopadhyay A, Aswarth PB (1997) J Mater Sci 32:2021. doi:10.1023/A:1018554217839
24. Horng HL, Jow LH (2002) J Am Ceram Soc 89:2331
25. Hirao K, Ohashi M, Brito ME, Kanzaki S (1995) J Am Ceram Soc 78:1687. doi:10.1111/j.1151-2916.1995.tb08871.x
26. Jais US, Lee WE, James PF (1999) J Am Ceram Soc 82:3200
27. Becher PF, Sun EY, Plucknett KP, Alexander KB, Hsueh CH, Lin HT et al (1998) J Am Ceram Soc 81:2821
28. Wang CM, Pan XQ, Ruhle M, Riley FL, Mitomo M (1996) J Mater Sci 31:5281. doi:10.1007/BF01159294
29. Horng HL, Jow LH (2001) J Am Ceram Soc 84:1891
30. Ye F, Chen S, Iwasa M (2003) Scr Mater 48:1433. doi:10.1016/S1359-6462(03)00083-6
31. Ziegler G, Heinrich J, Wotting G (1987) J Mater Sci 22:3041. doi:10.1007/BF01161167
32. Taya M, Hayashi S, Kobayashi AS, Yoon HS (1990) J Am Ceram Soc 73:1382. doi:10.1111/j.1151-2916.1990.tb05209.x